Acta Tecnología - International Scientific Journal about Technologies
Volume: 10 2024 Issue: 2 Pages: 57-64 ISSN 2453-675X

https://doi.org/10.22306/atec.v10i2.200 Received: 06 Apr. 2024; Revised: 12 May 2024; Accepted: 29 May 2024

Investigating the feasibility of energy harvesting from the third pedal in automotive systems using a mechanical motion rectifier: simulation-based study

Mohammed Alaa Alwafaie
István Sályi Doctoral School of Mechanical Engineering Sciences, Egyetem út 1, 3515, Miskolc, Hungary, EU,
alwafaie.mohammad.alaa@student.uni-miskolc.hu (corresponding author)
Bela Kovacs
István Sályi Doctoral School of Mechanical Engineering Sciences, Egyetem út 1, 3515, Miskolc, Hungary, EU,
matmn@uni-miskolc.hu

Keywords: energy harvesting, mechanical motion rectifier, simulation, electrical power generation.
Abstract: Automotive vehicles provide opportunities for energy harvesting from the mechanical motion generated during driving. In this study, we propose a novel design for a mechanical motion rectifier (MMR) that can generate electrical power from the mechanical motion of the third pedal in manual transmission vehicles. Using simulation and design tools, we investigate the feasibility of this system and explore the potential benefits and challenges of implementing it in automotive vehicles. Our results show that the proposed MMR system can effectively convert the oscillatory motion of the third pedal into unidirectional motion, which can then be used to generate electrical power. We also demonstrate that the design and operating parameters of the MMR system significantly impact its efficiency and performance. Our findings provide insights into the design and optimization of MMR systems for energy harvesting in automotive vehicles and highlight the potential for this technology to contribute to sustainable energy solutions.

1 Introduction

The quest for environmentally friendly and cost-effective energy solutions has fueled considerable improvements in the field of energy harvesting. Energy harvesting from mechanical motion has gained popularity as a possible method of producing electrical power in a variety of applications. The mechanical motion caused by driving gives an opportunity to utilize this energy source in the context of automobiles [1-3]. While driving, the third pedal frequently oscillates when pressure is applied to either the brake pedal or the throttle pedal. This oscillation is caused by a rod that connects both pedals. If effectively converted into electrical power, this movement could serve as a supplementary or alternative power source for automotive systems. The figure 1 shows a schematic of the mechanical motion transformation MMR for the third pedal [4].

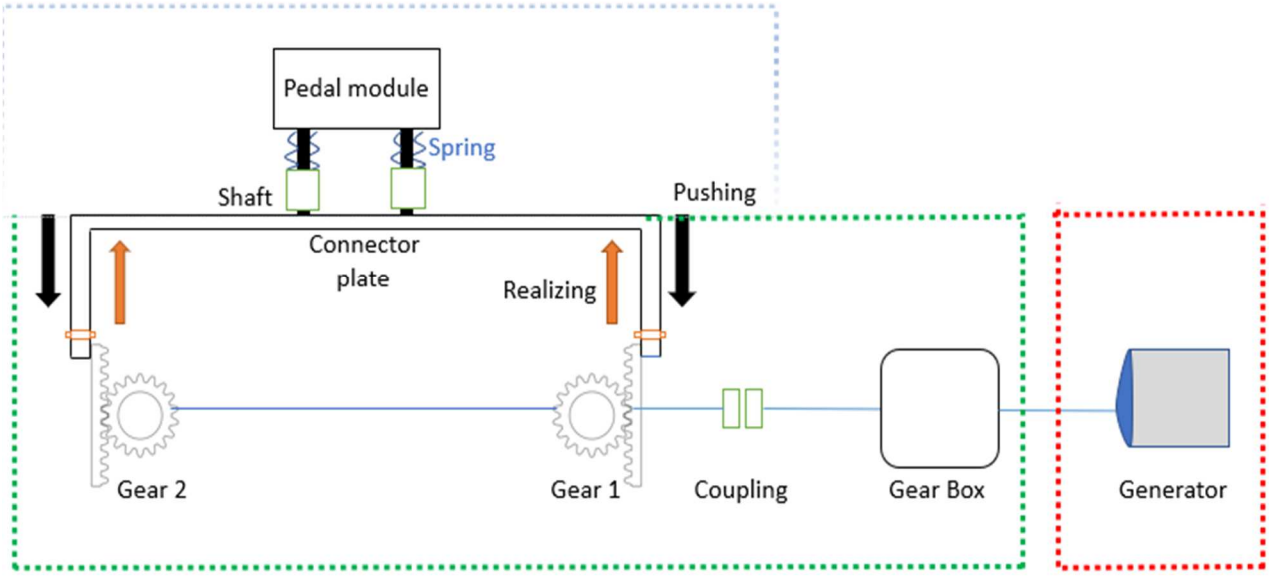

Figure 1 A schematic of the mechanical motion transformation MMR for the third pedal [4]

Investigating the feasibility of energy harvesting from the third pedal in automotive systems using a mechanical motion rectifier: simulation-based study

Mohammed Alaa Alwafaie, Bela Kovacs

The MMR achieves the conversion of linear motion from racks into rotational motion by interlocking pinion gears 1 and 2. When the driver vertically presses the pedal module, the rack moves, causing the pinion gear to rotate and the shaft to spin. This rotation of the shaft drives the gearbox, which in turn rotates the DC motor, generating electric power. To enhance power generation efficiency, a gearbox is utilized to increase rotational speed, as the linear motion of the rack alone cannot achieve high speeds. The generated energy is stored in a battery and can be used to recharge the vehicle at a later time.

2 Statistical analysis

To start statistical modeling, it is better to have an understanding of the various dynamics of the mechanical motion transformer MMR. This is crucial in investigating the feasibility of energy harvesting from the third pedal and demonstrating how we can control and extract power from this strategy.

2.1 Pedal harvesting energy dynamics

Pedal harvesting energy is a concept that involves utilizing the mechanical motion of a pedal, such as in a vehicle or a bicycle, to generate and harvest energy. In this context, the pedal serves as a means to convert mechanical force into usable energy [5-10].

Figure 2 illustrates the system of pedal harvesting energy, highlighting the pressed force acting on the pedal (PHE). This force is typically applied by the user, whether through their foot or another means of interaction. Understanding how this force is transmitted and translated within the system is crucial in analyzing the dynamics of pedal harvesting energy. It is important to understand how the pedal interacts with the mechanical motion transformer (MMR) as it plays a key role in determining the torque exerted on it.

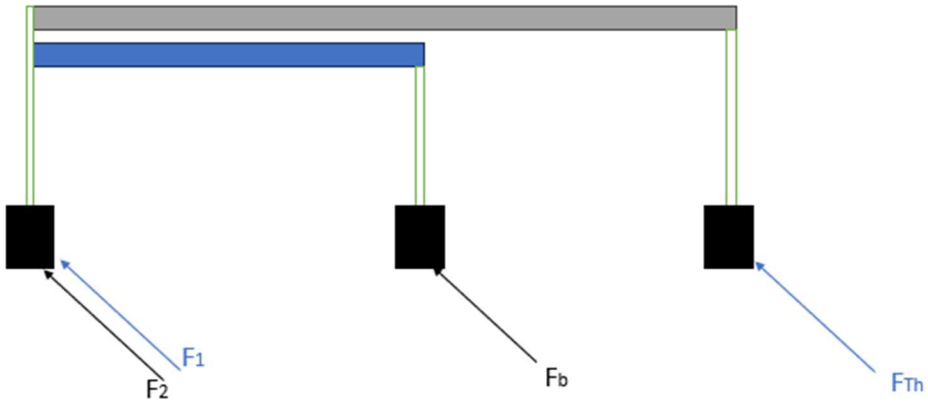

$F_{b:}$ The pressed force from the brake pedal,
F_{Th}: The pressed force from the throttle pedal,
F_1 & F_2: Forces that come from pressing the throttle and brake pedals separately.

Figure 2 The pressed force acting on the pedal (PHE)

The connection between the PHE (Pedal Harvesting Energy) system and the MMR (Mechanical Motion Transformer) system can be established through the consideration of spring stiffness and equivalent electrical damping as shown in figure 3. Spring stiffness K_b refers to the stiffness or resistance offered by a spring when it is compressed or stretched. In the context of the PHE and MMR system, the spring stiffness can be used to control the interaction between the pedal and the mechanical motion transformer. It determines the amount of force required to compress or stretch the spring, thereby affecting the torque and power transmission within the system. Equivalent electrical damping C_b refers to the damping effect that can be represented by an electrical circuit equivalent to the mechanical system. It is used to model the dissipation of energy within the system due to factors such as friction, air resistance, or other forms of mechanical damping.

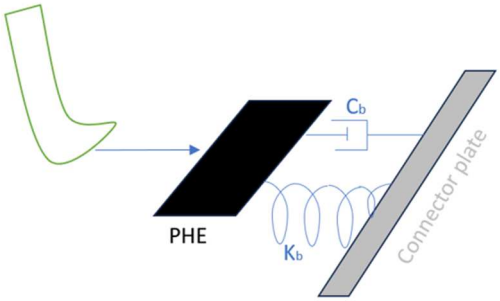

Figure 3 The connection between the PHE and the MMR by C_b, K_b

By incorporating equivalent electrical damping, the behavior and response of the system can be analyzed and optimized. The spring stiffness and equivalent electrical damping are parameters that can be adjusted and optimized to achieve desired performance characteristics in the PHE and MMR system. They play a role in determining factors such as the system's response time, stability, energy efficiency, and overall performance [11-14].

Based on Newton's second law of motion, we can write the equation of motion for the PHE (Pedal Harvesting Energy) system as follows (1), (2):

$$Mb\,.\,\ddot{x} + Cb\,.\,\dot{x} + kb.x = F_1 + F_2 \quad (1)$$

$$Mb\,.\,\ddot{x} + Cb\,.\,\dot{x} + kb.x = F_t \quad (2)$$

2.2 Dynamics equations for rack in MMR

The dynamic's equation for rack may describe based on Newton second law and according on figure 4 as follow (3), (4):

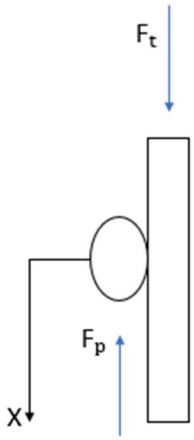

Figure 4 The forces acting on rack of MMR

$$M_r\,.\,a = F \quad (3)$$

$$M_r\,.\,\ddot{x} = -F_p + F_t \quad (4)$$

Also, the force of pinion gear can give as (5), (6):

$$F_p = \frac{2\pi T_p}{p\,\eta\,R} = K\frac{T_p}{R} \quad (5)$$

T_p: torque of pinion gear,
P: pitch of pinion,
η: efficiency of pinion,
R: the radius of pinion.

$$M_r\,.\,\ddot{x} + K\frac{T_p}{R} = F_t \quad (6)$$

2.3 Dynamics equations for pinion and outer ring of one-way clutch in MMR

In order to determine the equation for the given situation involving the MMR (Multi-Mass Rotor), it is necessary to sketch the torques and inertia associated with the system. To begin, a sketch of the MMR should be created, clearly indicating the positions of the angular displacement and the axis of rotation as in figure 5.

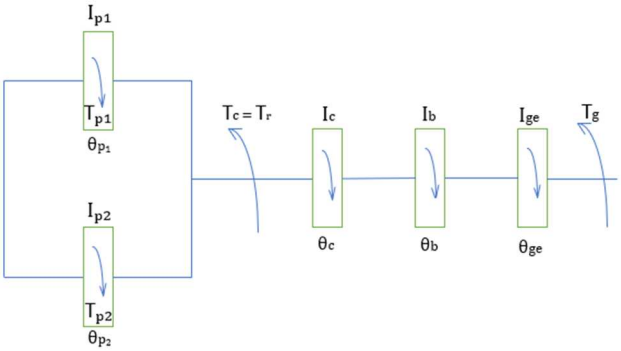

Figure 5 The moment of inertia and torques of MMR

Next, the moment of inertia for the MMR must be considered. The moment of inertia represents the rotational inertia of the system and is influenced by the distribution of masses and their distances from the axis of rotation. The total moment of inertia for the MMR can be obtained by summing the individual moments of inertia for each mass (7).

$$I = \int r^2.dm \quad (7)$$

dm: Differentiation mass for each part,
r: Distance for each part from axis of rotation.

The equation for the given situation can be derived by applying Newton's second law for rotational motion. This equation relates the net torque acting on the system to the moment of inertia and the angular acceleration of the MMR, so that for pinion allows us to analyze the rotational dynamics as follows (8), (9):

$$I_{p,n}\,.\,\ddot{\theta}_{p,n} = T_p - T_r \quad (8)$$

n = 1.2 because we have here in this case only two pinion gear.
$T_r = T_c$: The prevents rotation torque due to the presence of external loads or disturbances acting on the ring.

$$I_{p,n}\,.\,\ddot{\theta}_{p,n} = T_p - Tc \quad (9)$$

For the ring (10):

$$I_0\,.\,\ddot{\theta}_0 = -T_p \quad (10)$$

2.4 Dynamics equations for coupling, gearbox and generator in MMR

Depending on the moment of inertia and figure 5 we can determine each of dynamic equations for (11), (12):

1- Coupling

$$Ic\,.\,\ddot{\theta}c = Tc \quad (11)$$

2- Gearbox and generator

$$Ige\,.\,\ddot{\theta}ge + Ic\,.\,\ddot{\theta}c = Tc - Tg \quad (12)$$

$\theta_c = \theta_b = \theta$, $\theta_{ge} = n.\theta_b$ (n the ratio of gearbox) we can write (13):

$$Ige\,.n.\ddot{\theta}b + Ic\,.\ddot{\theta}b = Tc - Tg$$
$$(Ige\,.n + Ic\,)\ddot{\theta}b = Tc - Tg \quad (13)$$

Electromagnetic induced torque (T_g):

This torque produced by the interplay of electric currents and magnetic fields in a spinning electrical machine, such as generator and it gives as (14):

$$Tg = K_t\,.B\,.I.\sin\alpha \quad (14)$$

K_t is a constant factor that depends on the specific design of the machine.
B represents the strength of the magnetic field.
I represent the current flowing through the machine.
α is the angle between the magnetic field and the current.

In a simplified design scenario where there is a linear relationship between the torque and current, we can set α to 90° (indicating that the magnetic field and current are perpendicular) and assume B to be equal to 1 (representing a unit magnetic field strength). In this simplified case, the equation for the torque becomes (15):

$$Tg = K_t\,.I \quad (15)$$

This simplified design allows for a straightforward relationship between the torque and current, where the torque is directly proportional to the current. However, it's important to note that in practical electrical machines, the relationship between torque and current can be more complex and dependent on various factors such as the machine's design, magnetic field strength, and operating conditions.

From each of equations 6,9,13 we can analysis the equation for harvesting energy as following (16)-(23):

$$M_r\,.\ddot{x} + K\frac{T_p}{R} = F_t \quad (16)$$
$$M_r\,.r.\ddot{\theta} + K\frac{T_p}{R} = F_t \quad (17)$$
$$I_{p,n}\,.\ddot{\theta}_{p,n} = T_p - Tc \quad (18)$$
$$T_p = I_{p,n}\,.\ddot{\theta}_{p,n} + Tc \quad (19)$$
$$(Ige\,.n + Ic\,)\ddot{\theta}b + Tg = Tc \quad (20)$$
$$T_p = I_{p,n}\,.\ddot{\theta} + (Ige\,.n + Ic\,)\ddot{\theta} + Tg \quad (21)$$
$$T_p = (I_{p,n} + Ige\,.n + Ic\,)\ddot{\theta} + Tg \quad (22)$$
$$M_r\,.r.\ddot{\theta} + \frac{K}{R}(I_{p,n} + Ige\,.n + Ic\,)\ddot{\theta} + \frac{K}{R}.Tg = F_t \quad (23)$$

From equation 15 we can write (24):

$$M_r\,.r.\ddot{\theta} + \frac{K}{R}(I_{p,n} + Ige\,.n + Ic\,)\ddot{\theta} + \frac{K}{R}.K_t\,.I = F_t \quad (24)$$

The voltage (V) and current (I) for generator:

The electromotive voltage (EMF) in generator which connected by gearbox express by (25):

$$E = V = Kg.N.B.A.\omega \quad (25)$$

K_g: gear ratio and it is equal to n.
N: the number turn of coil inside the generator.
A: the area of coil.
ω: the out speed from gearbox.

We can express the voltage in another formula (26):

$$V = n.N.\dot{\theta} \quad (26)$$

Also, the current can write as (27)-(32):

$$I = V/R_t \quad (27)$$
$$I = \frac{n.N.\dot{\theta}}{R_t} \quad (28)$$
$$M_r\,.r.\ddot{\theta} + \frac{K}{R}(I_{p,n} + Ige\,.n + Ic\,)\ddot{\theta} + \frac{K}{R}.K_t\,.\frac{n.N.\dot{\theta}}{R_t} = F_t \quad (29)$$
$$[M_r\,.r + \frac{K}{R}(I_{p,n} + Ige\,.n + Ic\,)]\ddot{\theta} + [\frac{K.K_t\,.n.N}{R.R_t}]\dot{\theta} = F_t \quad (30)$$
$$M_e\,.\ddot{\theta} + C_e\,.\dot{\theta} = F_t \quad (31)$$
$$\ddot{\theta} = \frac{1}{M_e}F_t - \frac{C_e}{M_e}.\dot{\theta} \quad (32)$$

2.5 *The state of disengagement equation*

Upon disengagement of a system, the mechanical linkage between the driving force and the generator shaft is disrupted. Consequently, the generator shaft persists in its rotational motion owing to its inertia, although this motion experiences a progressive decay as time elapses. So, the angular displacement of the generator can describe as (33):

$$\dot{\theta}ge = \dot{\theta}ge\,.e^{-\alpha t} \quad (33)$$

$\alpha = C_e/M_e$ it is the decay factor, also known as the angular damping coefficient, controls the rate at which the generator shaft's rotational motion decreases.
t: this is the amount of time that has passed since the system was disconnected. The decay effect causes the angular displacement to decrease with time.

Based on equations (1), (32) and (33), it has been determined that the harvesting of energy can be achieved. The power can be calculated either from the angular velocity ($\dot{\theta}$) or from the linear velocity ($\dot{x}$) as follows (34):

$$P = Tg\,.\dot{\theta} = K_t\,.I\,.\dot{\theta} = K_t\,.I\,.\dot{x}/R = C_e\,.\dot{\theta}^2 \quad (34)$$

3 Modeling and experiment of MMR

To evaluate the effectiveness of MMR, an initial study was conducted to harvest energy from this technology. Additionally, to identify the factors that influence this energy harvest, it is necessary to determine the variable factors [15-17]. From the equation (1) we can found the pedal position as (35):

$$\ddot{x} = \frac{1}{Mb}F_t - \frac{Cb}{Mb}\dot{x} - \frac{kb}{Mb}x \quad (35)$$

Investigating the feasibility of energy harvesting from the third pedal in automotive systems using a mechanical motion rectifier: simulation-based study

Mohammed Alaa Alwafaie, Bela Kovacs

From the ODE45 and also drawing the Simulink for two equation we can found as figure 6.

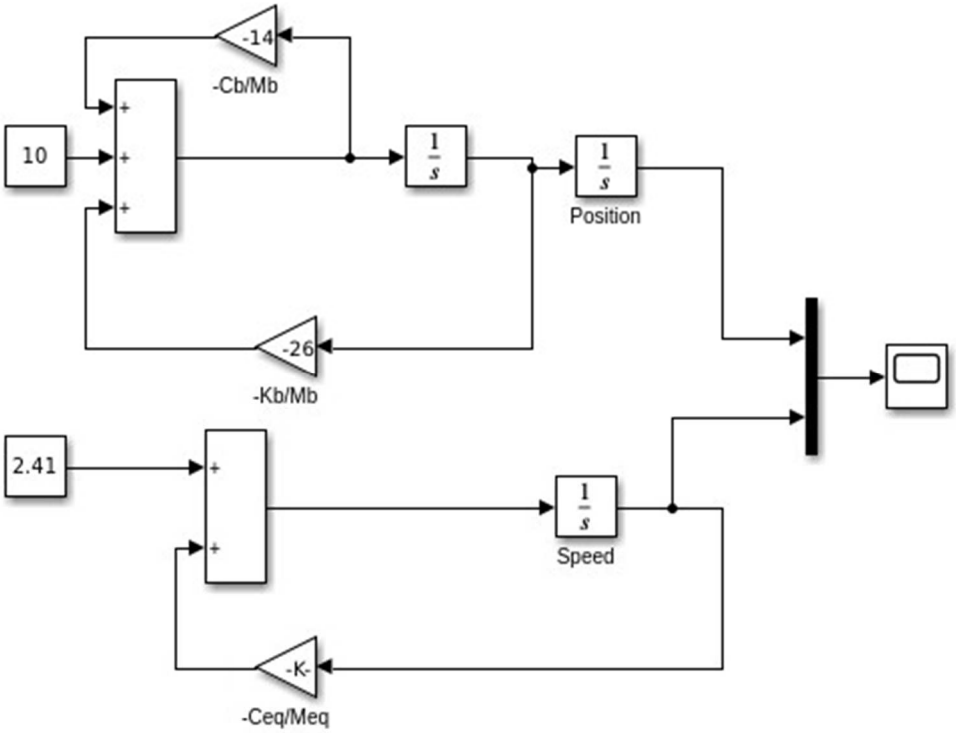

Figure 6 The drawing of Simulink for equation 1&32

The gain block comes from the indicators in the schedule (Table 1).

Table 1 The indicators for PHE

Name	Notation	Value and unit
Equivalent mass	Meq	207.25 kg
Pressing mass	Mb	50 kg
Equivalent coefficient when R_t =202Ω	Ceq	28.65 (N-s/m)
Pinion stiffness	K	0.5024 (N/m)
Generator stiffness	Kt	0.18 (N/m)
PHE stiffness	Kb	1300 (N/m)
PHE coefficient	Cb	700 (N-s/m)

Since (Ft) is related through (Mb) between the brake pedal and the throttle pedal according to equation (36), the value of each can be found according to scheme (Table 2).

$$F_t = \mathrm{Mb} \,.\, g \tag{36}$$

Table 2 The value of each brake and throttle pedal in small and big cars

Type	Small or family car	Big car
Brake pedal	(23- 45) kg	(45-68) kg
Throttle pedal	(9-23) kg	(23-45) Kg

To assess the effectiveness of MMR, an initial study was conducted to investigate the energy harvesting capabilities of this technology. Furthermore, in order to determine the factors that impact this energy harvest, specific values need to be identified. As depicted in Figure 7, the signals indicating the position of the pedal and the angular speed were examined over a period of approximately 60 seconds (one minute). The analysis revealed that the position of the pedal exhibited a linear relationship with time, steadily increasing. Conversely, the angular speed showed a gradual increase until reaching a peak of 17.5 radians.

Investigating the feasibility of energy harvesting from the third pedal in automotive systems using a mechanical motion rectifier: simulation-based study

Mohammed Alaa Alwafaie, Bela Kovacs

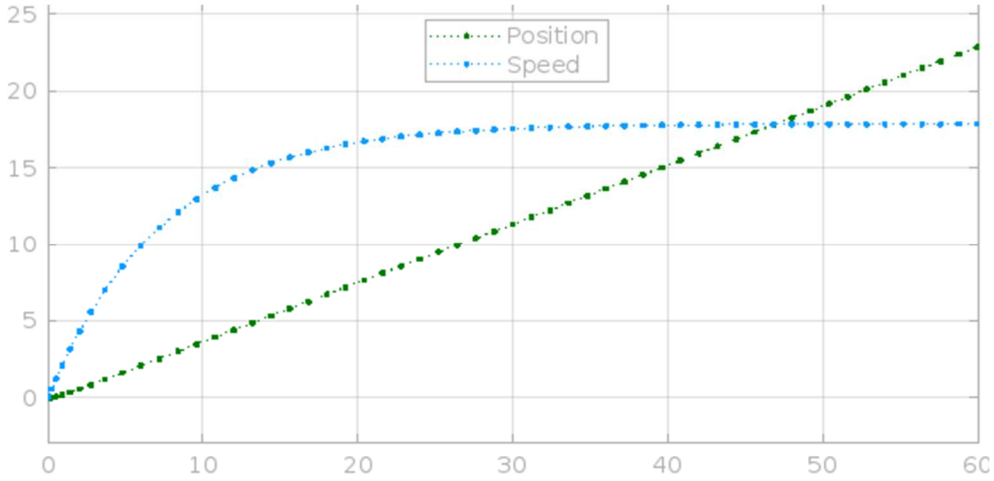

Figure 7 The position and angular speed plots to time

We can then perform a simulation according to equation (33) between the generator shaft in the left figure 8 and the pinion gear in the right figure 8 using six seconds of angular velocity (in radians) for two speed 3.21& 8.04 KMH of car speed (Figure 9).

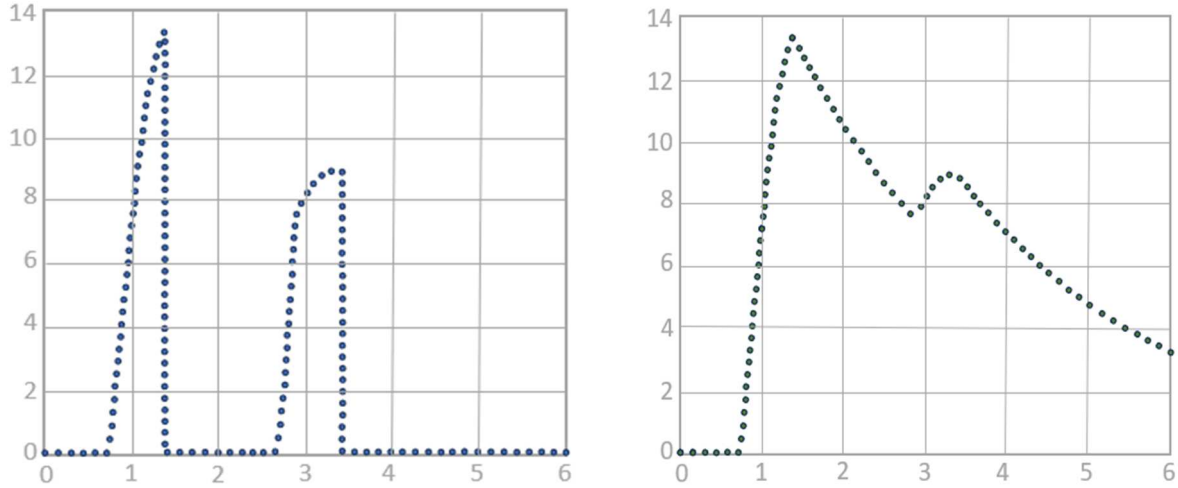

Figure 8 The position and angular speed plots to time for 3.21KMH of car speed

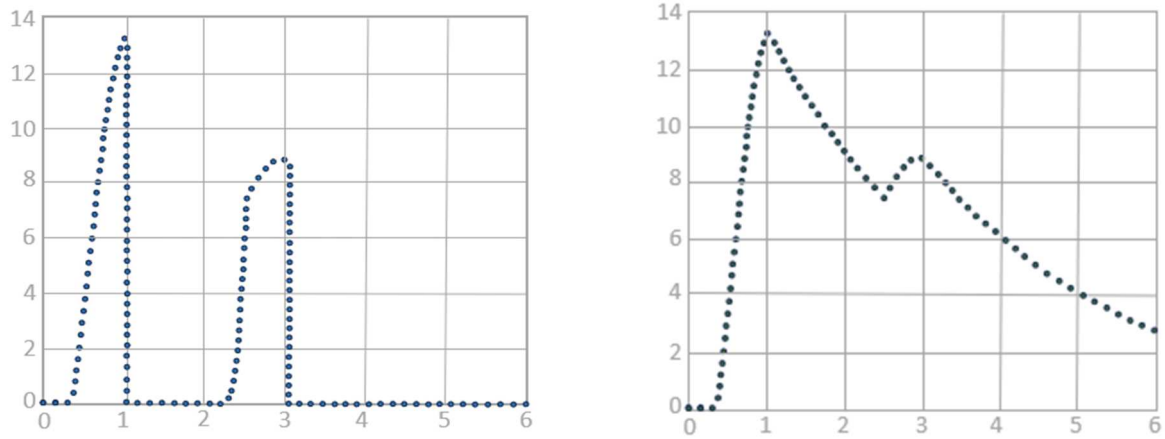

Figure 9 The position and angular speed plots to time for 8.04 KMH of car speed

The process of association and MMR dissociation is clearly visible in pervious graphs. As the vehicle begins to accelerate on the throttle pedal, the PHE descends and touches the rack and pinion assembly. Therefore, the system uses a pinion gear that drives the generator shaft at the same angular velocity. Once the lower limit of the rack is reached, the pinion releases and its angular velocity suddenly decreases to zero. After that, the system cuts off and the generator shaft continues to rotate with the decay factor (α) according to equation 33.

Since the generated power is directly proportional to the square of the angular velocity of the generator shaft, the same trend is followed the second peak observed in the figure indicated that the system engaged in retrieval process. Another thing we notice here is that as the speed of the car increases, the peaks will get closer. This makes sense because, at high speeds, the person's foot stays on the throttle pedal and moves lower and lower. So, the closure coming to the summit is a validation of that. Also pressing the brake pedal will be done when there is an emergency that needs to be pressed and using the same procedure as described before. on 202Ω we can found the power in figure 10.

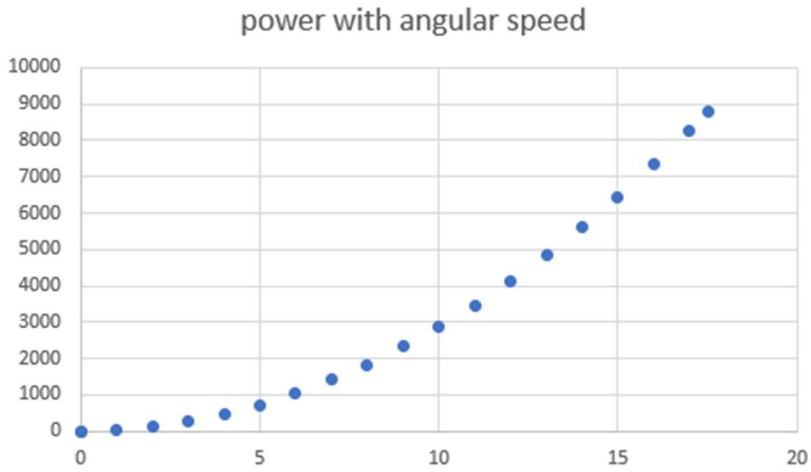

Figure 10 The power with angular speed at 202 Ω

The effect of external loads on energy production will support the simulation. To determine the energy harvested by this method it is advisable to test the different resistance connected to the generator as it gives us knowledge about the current. The simulation was conducted at a speed of 11.26 -16.09 km/h. We saw in figure 11 that we have two of the pressure peaks at PHE and generating power for R=110 Ω gives about 1145 watts for the first peak and about 735 watts for the second peak.

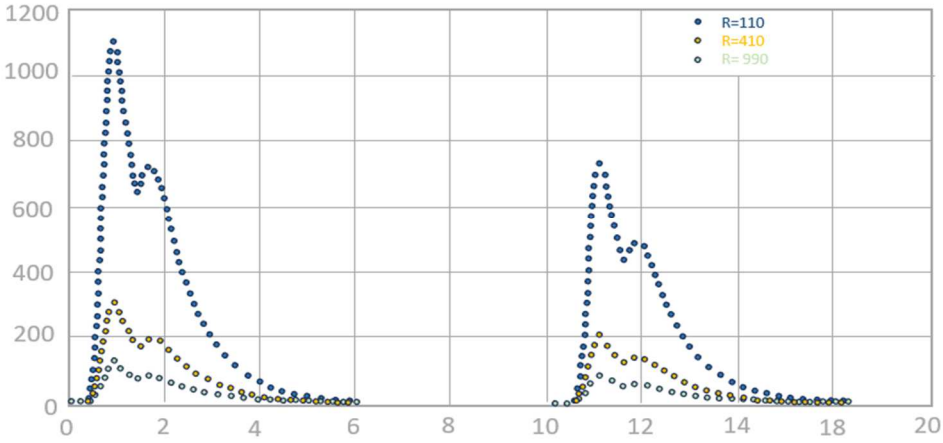

Figure 11 The generating power with time and different resistance

4 Conclusion

In this work, alternative energy harvesting has been investigated and developed using scientific method and technique. The pedal harvester and its geometry have been thoroughly studied, and a method for large scape electrical harvesting has been proposed. The ability of the pedal

energy harvester to generate electricity is determined by simulations field tests A MATLAB model has been developed to analyze the simulation results and the developed pedal energy harvester prototype has the ability to approximate 1100 watts of peak current. The proposed pedal power collector is expected to provide enough power for signals, monitoring sensors and It is very important to recharge the battery of the electric car. This means, the current prototype is a pioneering design of future designs of the same pedal harvester. This research opens a new area of research and invites researchers and engineers to work on it.

References

[1] VARAIYA, P.P.: Smart cars on smart roads: problems of control, *IEEE Transactions on Automatic Control*, Vol. 38, No. 2, pp. 195-207, 1991.

[2] MALIK, J., WEBER, J., LUONG, Q.-T., KOLLER, D.: *Smart cars and smart roads*, Proceedings of the British Machine Vision Conference, Birmingham, UK, pp. 367-382, 1995. http://dx.doi.org/10.5244/C.9.37

[3] KARPIRISKI, M., SENART, A., CAHILL, V.: *Sensor networks for smart roads*, Fourth Annual IEEE International Conference on Pervasive Computing and Communications Workshops (PERCOMW'06), Pisa, Italy, pp. 5-310, 2006. http://dx.doi.org/10.1109/PERCOMW.2006.123

[4] ALWAFAIE, M.A., KOVACS, B.: The mechanism parts of mechanical motion rectifier to produce energy from third pedal in automotive, *Acta Technologia*, Vol. 9, No. 2, pp. 73-77, 2023. https://doi.org/10.22306/atec.v9i2.174

[5] TANG, X., ZUO, L.: Vibration energy harvesting from random force and motion excitations, *Smart Materials and Structures*, Vol. 21, No. 7, pp. 1-9, 2012. http://dx.doi.org/10.1088/0964-1726/21/7/075025

[6] LI, Z., ZUO, L., LUHRS, G., LIN, L., QIN, Y.: Electromagnetic Energy-Harvesting Shock Absorbers: Design, Modeling, and Road Tests, *IEEE Transactions on Vehicular Technology*, Vol. 62, No. 3, pp. 1065-1074, 2013. http://dx.doi.org/10.1109/TVT.2012.2229308

[7] SARMA, B.S., JYOTHI, V., SUDHIR, D.: Design of Power Generation Unit Using Roller Mechanism, *IOSR Journal of Electrical and Electronics Engineering*, Vol. 9, No. 3, pp. 55-60, 2014.

[8] HILL, D., AGARWAL, A., TONG, N.: Assessment of piezoelectric materials for roadway energy harvesting, Cost of Energy and Demonstration Roadmap, Final project report, [Online], Available: http://pop.h-cdn.co/assets/cm/15/06/54d152f0cee9f_-_CEC-500-2013-007.pdf [20 Feb 2024], 2014.

[9] XIONG, Q., QIN, B., LI, X., ZUO, L.: *A Rule-Based Damping Control of MMR-Based Energy-Harvesting Vehicle Suspension*, 2020 American Control Conference (ACC), Denver, CO, USA, pp. 2262-2267, 2020. http://dx.doi.org/10.23919/ACC45564.2020.9147421

[10] WANG, L., TODARIA, P., PANDEY, A., O'CONNOR, J., CHERNOW, B., ZUO, L.: An electromagnetic speed bump energy harvester and its interactions with vehicles, *IEEE/ASME Transactions on Mechatronics*, Vol. 21, No. 4, pp. 1985-1994, 2016. http://dx.doi.org/10.1109/TMECH.2016.2546179

[11] TODARIA, P., WANG, L., PANDEY, A., O'CONNOR, J., MCAVOY, D., HARRIGAN, T., CHERNOW, B., ZUO, L.: *Design, modeling and test of a novel speed bump energy harvester*, In: Proceedings SPIE 9435, Sensors and Smart Structures Technologies for Civil, Mechanical, and Aerospace Systems 2015, Vol. 9435, pp. 38-51, 2015. https://doi.org/10.1117/12.2084371

[12] LI, Z., ZUO, L., KUANG, J., LUHRS, G.: Energy-harvesting shock absorber with a mechanical motion rectifier, *Smart Materials and Structures*, Vol. 22, No. 2, pp. 1-10, 2012. https://doi.org/10.1088/0964-1726/22/2/025008

[13] WANG, L., PARK, J., ZHOU, W., BAN, J., ZUO, L.: On-Road Energy Harvesting From Running Vehicles, [Online], Available: https://rosap.ntl.bts.gov/view/dot/31201/dot_31201_DS1.pdf [20 Feb 2024], 2014.

[14] SALMAN, W., QI, L., ZHU, X., PAN, H., ZHANG, X., BANO, S., ZHANG, Z., YUAN, Y.: A high-efficiency energy regenerative shock absorber using helical gears for powering low-wattage electrical device of electric vehicles, *Energy*, Vol. 159, No. September, pp. 361-372, 2018. https://doi.org/10.1016/j.energy.2018.06.152

[15] TODARIA, P.: *Design, Modelling, and Test of an Electromagnetic Speed Bump Energy Harvester*, Virginia Polytechnic Institute and State University, Blacksburg, Virginia, 2016.

[16] AZAM, A., AHMED, A., HAYAT, N., ALI, S., KHAN, A.S., MURTAZA, G., ASLAM, T.: Design, fabrication, modelling and analyses of a movable speed bump-based mechanical energy harvester (MEH) for application on road, *Energy*, Vol. 214, No. January, p. 118894, 2021.

[17] ALI, A., AHMED, A., ALI, M., AZAM, A., WU, X., ZHANG, Z., YUAN, Y.: A review of energy harvesting from regenerative shock absorber from 2000 to 2021: advancements, emerging applications, and technical challenges, *Environmental Science and Pollution Research*, Vol. 30, No. 3, pp. 5371-5406, 2023.

Review process
Single-blind peer review process.